Journal of Applied Fluid Mechanics, Vol. 9, No. 1, pp. 61-69, 2016.
Available online at www.jafmonline.net, ISSN 1735-3572, EISSN 1735-3645.
DOI: 10.18869/acadpub.jafm.68.224.23707

Finite Difference Analysis of Thermal Radiation and MHD Effects on Flow past an Oscillating Semi-Infinite Vertical Plate with Variable Temperature and Uniform Mass Flux

R. Muthucumaraswamy[1†] and B. Saravanan[2]

[1]*Professorand Head, Department of Applied Mathematics, Sri Venkateswara College of Engineering, Irungattukottai 602117, Sriperumbudur Taluk, India*
[2]*Assistant Professor, Department of Applied Mathematics, Sri Venkateswara College of Engineering, Irungattukottai 602117, Sriperumbudur Taluk, India*

†Corresponding Author Email*: msamy@svce.ac.in*

(Received July 1, 2014; accepted December 19, 2014)

ABSTRACT

MHD and thermal radiation effects on unsteady flow past an oscillating semi-infinite vertical plate with variable surface temperature and uniform mass flux have been studied. The dimensionless governing equations are solved by an efficient, more accurate, unconditionally stable and fast converging implicit finite difference scheme. The effect of velocity, concentratiion and temperature profiles for different parameters like magnetic field , thermal radiation, Schmidt number, thermal Grashof number, mass Grashof number are studied. It is observed that the velocity decreases with increasing values of the magnetic field parameter or radiation parameter.

Keywords:MHD; Radiation; Isothermal; Vertical plate; Finite-difference; Variable temperature; Mass flux.

NOMENCLATURE

a^*	absorbtion constants
C'	species concentration in the fluid
C	dimensionless concentration
C'_w	concentration of the plate
C'_∞	concentration in the fluid far away from the plate
C_p	specific heat at constant pressure
D	mass diffusion coefficient
Gc	mass Grashof number
Gr	thermal Grashof number
g	acceleration due to gravity
k	thermal conductivity
R	thermal radiation parameter
Pr	Prandtl number
Sc	Schmidt number
M	magnetic field parameter
Nu_x	dimensionless local Nusselt number
$\overline{Nu}$	dimensionless average nusselt number
Sh_x	dimensionless local Sherwood number
$\overline{Sh}$	dimensionless average Sherwood number
u,v	velocity of the components of the fluid in X, Y-directions respectively
x	coordinate along the plate
y	coordinate axis normal to the plate
X	dimensionless coordinate along the plate
Y	dimensionless coordinate axis normal to the plate
α	thermal difusivity
β	volumetric coefficient of thermal expansion
β^*	volumetric coefficient of expansion with concentration
μ	coefficient of viscosity
ω'	frequency of oscillation
ω	dimensional frequency of oscillation
$\omega' t'$	phase angle
ωt	dimensional phase angle
ν	kinematic viscosity

T	temperature of the fluid near the plate
T'	temperature
T_w	temperature of the plate
T_∞	temperature of the fluid far away from the plate
t'	time
u_0	velocity of the plate
σ	electric conductivity
ρ	density of the fluid
θ	dimensionless temperature
τ_x	**dimensionless local skin friction**
$\bar{\tau}$	dimesionless average skin friction
w	conditions at the wall
∞	free stream conditio

1. INTRODUCTION

MHD plays an important role in agriculture,petroleum industries, geophysics and in astrophysics. Important applications in the study of geological formations, in exploration and thermal recovery of oil,and in the assessment of aquifers,geothermal reservoirs and underground nuclear waste storage sites. MHD finds applications in electromagnetic pumps, controlled fusion research, crystal growing, MHD couples and bearings, plasma jets, chemical synthesis and MHD power generators

MHD flow has application in metrology, solar physics and in motion of earths core. Also it has applications in the field of stellar and planetary magnetospheres, aeronautics, chemical engineering and electronics. In the field of power generation, MHD is receiving considerable attention due to the possibilities it offers for much higher thermal efficiencies in power plants. Examples include magnetic control of molten iron flow in the steel industry, liquid metal cooling in nuclear reactors and magnetic suppression of molten semi-conducting materials

Soundalgekar,Patil, Jahagirdar(1981) have studied MHD Stokes problem for a vertical plate with variable temperature. Again Mass Transfer effect on the Flow Past an Oscillating Infinite Vertical Plate with Constant Heat Fluxstudied by Soundalgekar *et al*(1994). Muthucumaraswamy (2009)have analyzed MHD effects on flow past an infinite oscillating vertical plate in the presence of an optically thin gray gas. Soundalgekar and Akolkar(1983) have studied Effects of free convection currents and mass transfer on the flow past a vertical oscillating plate.

Raptis, Perdikis (1999) have analyzed Radiation and free convection flow past a moving plate. England and Emery (1969) have studied the thermal radiation effects of a optically thin gray gas bounded by a stationary vertical plate.Soundalgekar , Gupta and Aranake(1979) have analyzed Free convection currents on MHD Stokes problem for a vertical plate. Soundalgekar , Gupta and Birajdar (1979) have studied the Effects of Mass transfer and free convection currents on MHD Stokes problem for a vertical plate.

Radiation effect on mixed convection along a isothermal vertical plate were studied by Hossain and Takhar (1996). Raptis and Perdikis (2003) have studied the effects of thermal radiation of an optically thin gray gas. Free convection effects on the flow past a vertical oscillating plate was studied by Soundalgekar (1979). Shanker and Kishan (1997) have analyzed the effect of mass transfer on the MHD flow past an impulsively started infinite vertical plate with variable temperature or constant heat flux. MHD Stokes problem for a vertical infinite plate with variable temperature was studied by Soundalgekar, Patil and Jahagirdar(1981). Singh and Sacheti(1988) have studied the Finite difference analysis of unsteady hydromagnetic free-convection flow with constant heat flux.

Flow past an impulsively started vertical plate with constant heat flux and mass transfer were studied by Muthucumaraswamy and Ganesan(2000).Deka and Neog(2009) have analyzed the Unsteady MHD flow past a vertical oscillating plate with thermal radiation and variable mass diffusion. Finite difference analysis of radiative free convection flow past an impulsively started vertical plate with variable heat and mass flux studied by Prasad *et al*(2011). Palani and Srikanth(2009) have studied MHD flow past a semi-infinite vertical plate with mass transfer. Prasad, Reddy and Muthucumaraswamy (2007) have analyzed Radiation and mass transfer effects on two dimension flow past an impulsively started infinite vertical plate. Thermal radiation effects on MHD flow past a vertical oscillating plate were studied by Chandrakala,.Bhaskar(2009).

Rajput and Kumar (2011) have analyzed MHD flow past an impulsively started vertical plate with variable temperature and mass diffusion.

Unsteady free convection flow past an oscillating plate with constant mass flux in the presence of radiation were studied by Chaudhary and Jain(2007).

Muthucumaraswamy and Vijayalakshmi(2008) have studied Effects of heat and mass transfer on flow past an oscillating vertical plate with variabletemperature.Neog and Das Rudra (2012) have analyzed Unsteady Free Convection MHD flow past a vertical plate with variable temperature and chemical reaction. Radiation effects on MHD flow past an impulsively started vertical plate with variable heat and mass transfer were studied by Rajput and Kumar(2012).

Finite difference solution on natural convection along an oscillating isothermal vertical plate under the combined buoyancy effects of heat and mass diffusion in the presence of thermal radiation has not received attention of any researcher. This study found useful in distribution of cooling in a closed environment. Hence, the present study is to investigate the unsteady flow past an oscillating semi-infinite vertical plate with thermal radiation by an implicit finite-difference scheme of Crank-Nicolson type.

2. MATHEMATICAL FORMULATION OF THE PROBLEM

A transient, laminar, unsteady natural convection flow of a viscous incompressible fluid past an oscillating semi-infinite isothermal vertical plate in the presence of thermal radiation has been considered. It is assumed that the concentration C' of the diffusing species in the binary mixture is very less in comparison to the other chemical species which are present. Here, the *x*-axis is taken along the plate in the vertically upward direction and the *y*-axis is taken normal to the plate. The physical model of the problem is shown in figure 1.

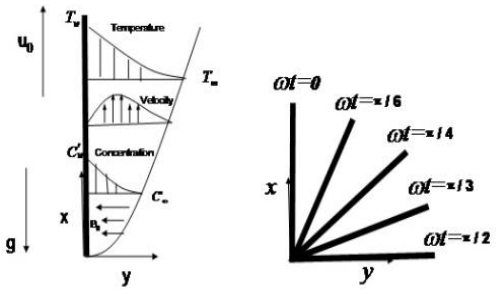

Fig. 1. Physical model of the problem.

Initially, it is assumed that the plate and the fluid are of the same temperature and concentration. At time $t' > 0$, the plate starts oscillating in its own plane with frequency ω' againstgravitational field. The temperature of the plate is raised $T_w(x)(=T_\infty + ax^n)$ and the concentrationlevelnear the plate is raised at a constant rate. The fluid considered here is a gray, absorbing-emitting radiation but a non-scatteringmediumand the viscous dissipation is assumed to be negligible. Then under the above assumptions, the governing boundary layer equations of mass, momentum and concentration for free convective flow withusual Boussinesq's approximation are as follows(Gebart and Pera(1971):

$$\frac{\partial u}{\partial x} + \frac{\partial v}{\partial y} = 0 \tag{1}$$

$$\frac{\partial u}{\partial t'} + u\frac{\partial u}{\partial x} + v\frac{\partial u}{\partial y} = g\beta(T' - T_\infty) + g\beta^*(C' - C'_\infty) + \nu\frac{\partial^2 u}{\partial y^2} - \frac{\sigma B_\circ^2}{\rho}u \tag{2}$$

$$\rho C_p\left(\frac{\partial T'}{\partial t'} + u\frac{\partial T'}{\partial x} + v\frac{\partial T'}{\partial y}\right) = k\frac{\partial^2 T'}{\partial y^2} - \frac{\partial q_r}{\partial y} \tag{3}$$

$$\frac{\partial C'}{\partial t'} + u\frac{\partial C'}{\partial x} + v\frac{\partial C'}{\partial y} = D\frac{\partial^2 C'}{\partial y^2} \tag{4}$$

The initial and boundary conditions are

$$t' \le 0 : u = 0,\ v = 0, T' = T_\infty, C' = C'_\infty$$

$$t' > 0 : \left.\begin{array}{l} u = u_0\cos\omega' t',\ v = 0, \\ T' = T_\infty + ax^n,\ \dfrac{\partial C'}{\partial y} = -\dfrac{j''}{D} \end{array}\right\} at\ y = 0$$

$$u = 0,\ T' = T_\infty,\ C' = C'_\infty \quad at\ \ x = 0$$

$$u \to 0,\ T' \to T_\infty,\ C' \to C'\ as\ \ y \to \infty \tag{5}$$

In the case of an optically thin gray gas the local radiant absorption is expressed by

$$\frac{\partial q_r}{\partial y} = -4a^*\sigma\left(T_\infty^4 - T'^4\right) \tag{6}$$

We assume that the temperature differences within the flow are sufficiently small such that T'^4 may be expressed as a linear function of the temperature. This is accomplished by expanding T'^4in a Taylor series about T_∞ and neglecting higher-order terms, thus

$$T'^4 \cong 4T_\infty^3 T' - 3T_\infty^4 \tag{7}$$

By using equations (6) and (7), equation (3) reduces to

$$\rho C_p\left(\frac{\partial T'}{\partial t'} + u\frac{\partial T'}{\partial x} + v\frac{\partial T'}{\partial y}\right) = k\frac{\partial^2 T'}{\partial y^2} + 16a^*\sigma T_\infty^3(T_\infty - T') \tag{8}$$

On introducing the following non-dimensional quantities

$$U = \frac{u}{u_0},\ V = \frac{v\sqrt{L}}{\sqrt{u_0\nu}},\ t = \frac{t'u_0}{L},\ X = \frac{x}{L},$$

$$Y = \frac{y\sqrt{u_0}}{\sqrt{L\nu}},\ T = \frac{T' - T_\infty}{T_w(L) - T_\infty},$$

$$Gr = \frac{Lg\beta(T_w(L) - T_\infty)}{u_0^2},\ C = \frac{C' - C'_\infty}{\left(\frac{j''\sqrt{L\nu}}{D\sqrt{u_0}}\right)},$$

$$Gc = \frac{Lg\beta^*\left(\frac{j''\sqrt{L\nu}}{D\sqrt{u_0}}\right)}{u_0^2},$$

$$R = \frac{16a^*L\nu\sigma T_\infty^3}{k u_0},\ Pr = \frac{\nu}{\alpha},\ Sc = \frac{\nu}{D}$$

$$\omega' = \frac{\omega u_0}{L},\ M = \frac{\sigma B_\circ^2 L}{\rho u_\circ} \tag{9}$$

Equations (1) to (4) are reduced to the following non-dimensional form

$$\frac{\partial U}{\partial X} + \frac{\partial V}{\partial Y} = 0 \tag{10}$$

$$\frac{\partial U}{\partial t} + U\frac{\partial U}{\partial X} + V\frac{\partial U}{\partial Y} = Gr\,T + Gc\,C + \frac{\partial^2 U}{\partial Y^2} - MU \tag{11}$$

$$\frac{\partial T}{\partial t}+U\frac{\partial T}{\partial X}+V\frac{\partial T}{\partial Y}=\frac{1}{\Pr}\frac{\partial^2 T}{\partial Y^2}-\frac{R}{\Pr}T \tag{12}$$

$$\frac{\partial C}{\partial t}+U\frac{\partial C}{\partial X}+V\frac{\partial C}{\partial Y}=\frac{1}{Sc}\frac{\partial^2 C}{\partial Y^2} \tag{13}$$

The corresponding initial and boundary conditions in non-dimensional quantities are

t ≤ 0 : U =0,V = 0, T = 0, C =0

t > 0: U =*Cosωt*, V =0,

$$T=x^n,\ \frac{\partial C}{\partial Y}=-1 \text{ at } Y=0 \tag{14}$$

U = 0, T = 0, C = 0 at X = 0

U $\to$0, T $\to$0, C $\to$0 as Y $\to\infty$

3. NUMERICAL TECHNIQUE

In order to solve the unsteady, non-linear coupled equations (10) to (13) under the conditions (14), an implicit finite difference scheme of Crank-Nicolson type has been employed. The finite difference equations corresponding to equations (10) to (13) are as follows:

$$\frac{\left[U_{i,j}^{n+1}-U_{i-1,j}^{n+1}+U_{i,j}^{n}-U_{i-1,j}^{n}\right]}{4\Delta X}+\frac{\left[U_{i,j-1}^{n+1}-U_{i-1,j-1}^{n+1}+U_{i,j-1}^{n}-U_{i-1,j-1}^{n}\right]}{4\Delta X}+\frac{\left[V_{i,j}^{n+1}-V_{i,j-1}^{n+1}+V_{i,j}^{n}-V_{i,j-1}^{n}\right]}{2\Delta Y}=0 \tag{15}$$

$$\frac{\left[U_{i,j}^{n+1}-U_{i,j}^{n}\right]}{\Delta t}+U_{i,j}^{n}\frac{\left[U_{i,j}^{n+1}-U_{i-1,j}^{n+1}+U_{i,j}^{n}-U_{i-1,j}^{n}\right]}{2\Delta X}+V_{i,j}^{n}\frac{\left[U_{i,j+1}^{n+1}-U_{i,j-1}^{n+1}+U_{i,j+1}^{n}-U_{i,j-1}^{n}\right]}{4\Delta Y}=\frac{Gr}{2}\left[T_{i,j}^{n+1}+T_{i,j}^{n}\right]+\frac{Gc}{2}\left[C_{i,j}^{n+1}+C_{i,j}^{n}\right]-\frac{M}{2}\left[U_{i,j}^{n+1}+U_{i,j}^{n}\right]+\frac{\left[U_{i,j-1}^{n+1}-2U_{i,j}^{n+1}+U_{i,j+1}^{n+1}+U_{i,j-1}^{n}-2U_{i,j}^{n}+U_{i,j+1}^{n}\right]}{2(\Delta Y)^2} \tag{16}$$

$$\frac{\left[T_{i,j}^{n+1}-T_{i,j}^{n}\right]}{\Delta t}+U_{i,j}^{n}\frac{\left[T_{i,j}^{n+1}-T_{i-1,j}^{n+1}+T_{i,j}^{n}-T_{i-1,j}^{n}\right]}{2\Delta X}+V_{i,j}^{n}\frac{\left[T_{i,j+1}^{n+1}-T_{i,j-1}^{n+1}+T_{i,j+1}^{n}-T_{i,j-1}^{n}\right]}{4\Delta Y}=\frac{1}{Pr}\frac{\left[T_{i,j-1}^{n+1}-2T_{i,j}^{n+1}+T_{i,j+1}^{n+1}+T_{i,j-1}^{n}-2T_{i,j}^{n}+T_{i,j+1}^{n}\right]}{2(\Delta Y)^2}-\frac{R(T_{i,j}^{n+1}+T_{i,j}^{n})}{2Pr} \tag{17}$$

$$\frac{\left[C_{i,j}^{n+1}-C_{i,j}^{n}\right]}{\Delta t}+U_{i,j}^{n}\frac{\left[C_{i,j}^{n+1}-C_{i-1,j}^{n+1}+C_{i,j}^{n}-C_{i-1,j}^{n}\right]}{2\Delta X}+V_{i,j}^{n}\frac{\left[C_{i,j+1}^{n+1}-C_{i,j-1}^{n+1}+C_{i,j+1}^{n}-C_{i,j-1}^{n}\right]}{4\Delta Y}=\frac{1}{Sc}\frac{\left[C_{i,j-1}^{n+1}-2C_{i,j}^{n+1}+C_{i,j+1}^{n+1}+C_{i,j-1}^{n}-2C_{i,j}^{n}+C_{i,j+1}^{n}\right]}{2(\Delta Y)^2} \tag{18}$$

The concentration boundary condition at Y=0 in the finite difference form is

$$\frac{1}{2}\frac{\left[C_{i,1}^{n+1}+C_{i,1}^{n}-C_{i,-1}^{n+1}-C_{i,-1}^{n}\right]}{2\Delta Y}=-1 \tag{19}$$

At $Y=0$ (i.e., j=0) equation (18), becomes

$$\frac{\left[C_{i,0}^{n+1}-C_{i,0}^{n}\right]}{\Delta t}+U_{i,0}^{n}\frac{\left[C_{i,0}^{n+1}-C_{i-1,0}^{n+1}+C_{i,0}^{n}-C_{i-1,0}^{n}\right]}{2\Delta X}=\frac{1}{Sc}\frac{\left[C_{i,-1}^{n+1}-2C_{i,0}^{n+1}+C_{i,1}^{n+1}+C_{i,-1}^{n}-2C_{i,0}^{n}+C_{i,1}^{n}\right]}{2(\Delta Y)^2} \tag{20}$$

After eliminating $C_{i,-1}^{n+1}+C_{i,-1}^{n}$ using equation (19), equation (20) reduces to the form

$$\frac{\left[C_{i,0}^{n+1}-C_{i,0}^{n}\right]}{\Delta t}+U_{i,0}^{n}\frac{\left[C_{i,0}^{n+1}-C_{i-1,0}^{n+1}+C_{i,0}^{n}-C_{i-1,0}^{n}\right]}{2\Delta X}=\frac{1}{Sc}\frac{\left[C_{i,1}^{n+1}-C_{i,0}^{n+1}+C_{i,1}^{n}-C_{i,0}^{n}+2\Delta Y\right]}{(\Delta Y)^2} \tag{21}$$

Here the region of integration is considered as a rectangle with sides X_{max}(= 1) and Y_{max} (=20), where Y_{max} corresponds to $Y = \infty$ which lies very well outside both the momentum and energy boundary layers. The maximum of Y was chosen as 20 after some preliminary investigations so that the last two of the boundary conditions (14) are satisfied with in the tolerance limit 10^{-5}. After experimenting with a few set of mesh sizes have been fixed at the level $\Delta X = 0.05$, $\Delta Y = 0.25$, with time step $\Delta t = 0.01$. In this case, the spatial mesh sizes are reduced by 50% in one direction, and later in both directions, and the results are compared. It is observed that, when the mesh size is reduced by 50% in the *Y*-direction, the results differ in the fifth decimal place while the mesh sizes are reduced by 50% in *X*-direction or in both directions; the results are comparable to three decimal places. Hence, the above mesh sizes have been considered as appropriate for calculation. The coefficients $U_{i,j}^{n}$ and $V_{i,j}^{n}$ appearing in the finite difference equation are treated as constants at any one time step. Here *i*-designates the grid point along the *X* - direction, *j* along the *Y*- direction and *k* to the *t*-time. The values of *U, V* and *T* are known at all grid points at *t = 0* from the initial conditions.

The computations of *U, V* , *T* and *C* at time level (n +1) using the values at previous time level (n) are carried out as follows: The finite-difference equations (18) and (21) at every internal nodal point on a particular *i*-level constitute a tridiagonal system of equations. The system of equations is solved by using Thomas algorithm as discusses in Carnahan *et al* (1969). Thus, the values of *C* are

found at every nodal point for a particular *i* at $(n+1)^{th}$ time level. Similarly, the values of *T* arecalculated from equation (17) .Using the values of *C* and *T* at $(n+1)^{th}$ time level in the equation (16) , the values of *U* at $(n+1)^{th}$ time level are found in a similar manner. Thus, the values of *C*, *T* and *U* are known on a particular *i*-level. Finally, the values of *V* are calculated explicitly using the equation (15) at every nodal point at particular *i*-level at $(n+1)^{th}$ time level. This process is repeated for various *i*-levels. Thus the values of *C, T, U* and *V* are known, at all grid points in the rectangle region at $(n+1)^{th}$ time level.

In a similar manner computations are carried out by moving along i-direction. After computing values corresponding to each i at a time level, the values at the next time level are determined in a similar manner. Computations are repeated until the steady-state is reached. The steady-state solution is assumed to have been reached, when the absolute difference between the values of *U*, and as well as temperature *T* and concentration *C* at two consecutive time steps are less than 10^{-5} at all grid points.

4. RESULTS AND DISCUSSION

The numerical values of the velocity, temperature and concentation are computed for different parameters like radiation parameter, magnetic field, Schmidt number, phase angle, thermal Grashof number and mass Grashof number. The purpose of the calculations given here is to assess the effects of the parameters $\omega t, R, Gr, Gc$ and *Sc* upon the nature of the flow and transport. The value of Prandtl number Pris chosen such that they represent air (*Pr* = 0.71) and the Schmidt number Sc = 0.6(Water vapour).

The steady-state velocity profiles for different phase angle are shown in figure 2. The velocity profiles presented are those at X = 1.0. It is observed that for different phase angle ($\omega t = 0, \pi/6, \pi/3, \pi/2$), Gr=5=Gc, M=2 and R=2 the velocity decreases with increasing phase angle. Here ωt = 0 represents vertical plate and note that the velocity profile grows from *U* = 1 and $\omega t = \pi/2$ refers horizontal plate and the velocity profiles starting with *U* = 0. The numerical value satisfies with the prescribed boundary conditions. It is also observed that the time taken to reach steady-state is more in the case of vertical plate than horizontal plate. The trend shows that the contribution of mass diffusion is very dominant in the velocity field.

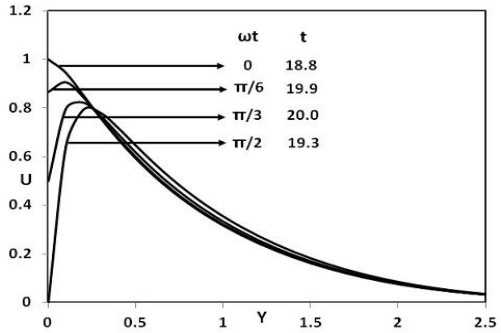

Fig. 2. steady state velocity profiles for different.

In figure 3, the velocity profiles for different thermal Grashof number(Gr=,5,10), mass Grashof number(Gc=5,10), $\omega t = \pi/6$, M=2 and R=2 are shown graphically. This shows that the velocity increases with increasing thermal Grashof number or mass Grashof number. As thermal Grashof number or mass Grashof number increases, the buoyancy effect becomes more significant, as expected; it implies that, more fluid is entrained from the free stream due to the strong buoyancy effects.

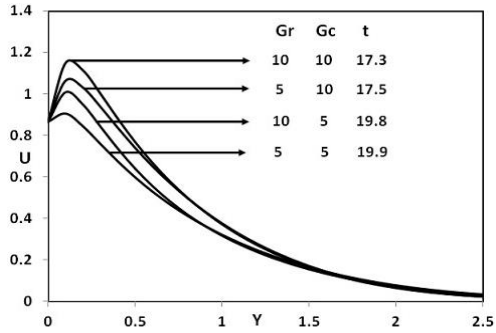

Fig. 3. Steady state velocity profiles for different values of Gr & Gc.

The effect of velocity for different radiation parameter (R = 0.2, 2, 5, 10), $\omega t = \pi/6$, M=2 and Gr=Gc=5 are shown in figure 4. It is observed that the velocity increases with decreasing radiation parameter. This shows that due to higher thermal radiation the velocity decreases tremendously. As expected, the heat loss is more in the presence of higher thermal radiation.

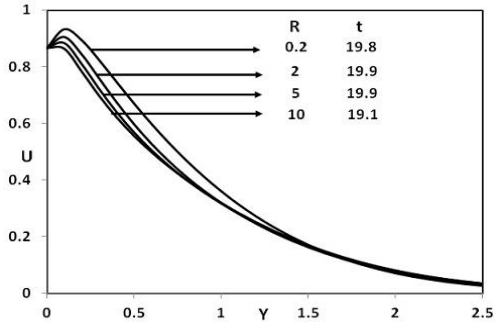

Fig. 4. Steady state velocity profiles for different values of R.

The steady state velocity profiles for different magnetic parameter are shown in figure 5. It is

observed that for (M=2, 5, 10), Pr=0.71, R=2 and Sc=0.6, the velocity decreases in the presence of magnetic field. This shows that the increase in the magnetic field parameter leads to a fall in the velocity. This agrees with expectation, since the magnetic field exerts a retarding force on free convection flow.

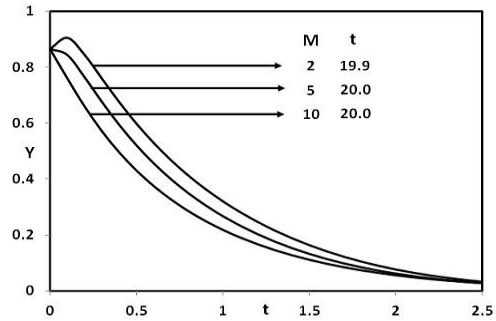

Fig. 5. Steady state velocity profiles for different values of M.

The steady-state velocity profiles for different Schmidt number (Sc=0.16,0.3,0.6,2.01), Gr=Gc=5, $\omega t = \pi/6$, M=2 and R=2 are shown in figure6. The velocity profiles presented are those at X = 1.0. It is observed that the velocity decreases with increasing Schmidt number and the steady-state value increases with increasing Schmidt number. The velocity boundary layer seems to grow in the direction of motion of the plate. It is observed that near the leading edge of a semi-infinite vertical plate moving in a fluid, the boundary layer develops along the direction of the plate. However, the time required for the velocity to reach steady-state depends upon the Schmidt number. This shows that the contribution of mass diffusion to the buoyancy force increases the maximum velocity significantly.

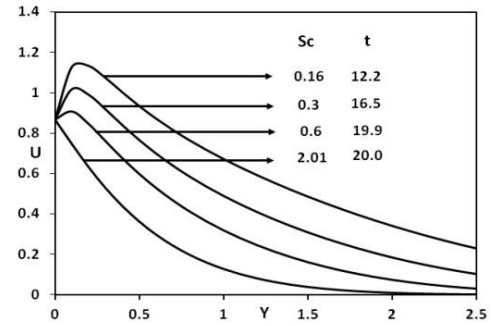

Fig. 6. Steady state velocity profiles for different values of Sc.

In all the above graphs(fig.2-fig.6), it is observed that the velocity increases near the plate and decreases far away from the plate. This is true because the velocity, temperature and concentrationeffects outside the boundary layer are negligible (Refer last boundary condition in (14))

The temperature profiles for different values of the thermal radiation parameter (R=0.2, 2, 5, 10) are shown in figure 7. It is observed that the temperature increases with decreasing R. This shows that the buoyancy effect on the temperature distribution is very significant in air (Pr = 0.71). It is clear that the steady state attained for R=0.2 at t=14.2 and R=10 at t=5.9. This shows that the time taken to reach steady state is more for lower thermal radiation parameter as compared to higher thermal radiation parameter. It is known that the radiation parameter and Prandtl number plays an important role in flow phenomena because, it is a measure of the relative magnitude of viscous boundary layer thickness to the thermal boundary layer thickness.

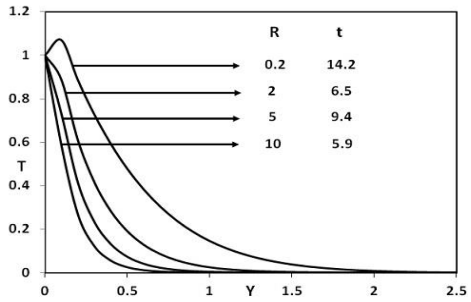

Fig. 7. Temperature profiles for different values of R.

The concentration profiles for different values of the Schmidt number (Sc=0.16, 0.3, 0.6, 2.01) are shown in figure 8. It is observed that the plate concentration increases with decreasing Sc. It is clear that steady state attained for Sc=0.16 at t=11.4 and Sc=2.01 at t=19.9. This shows that time taken to reach steady state is more for higher Schmidt number as compared to lower Schmidt number.

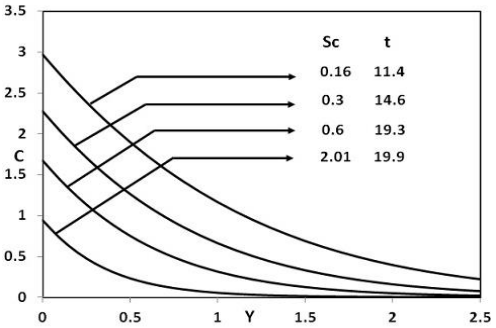

Fig. 8. Conecentration profiles for different values of Sc.

Knowing the velocity and temperature field, it is customary to study the skin-friction, Nusselt number and Sherwood number. The local as well as average values of skin-friction, Nusselt number and Sherwood number in dimensionless form are as follows:

$$\tau_X = -\left(\frac{\partial U}{\partial Y}\right)_{Y=0} \tag{22}$$

$$\bar{\tau} = -\int_0^1 \left(\frac{\partial U}{\partial Y}\right)_{Y=0} dX \tag{23}$$

$$Nu_X = \frac{-X\left(\frac{\partial T}{\partial Y}\right)_{Y=0}}{T_{Y=0}} \tag{24}$$

$$\overline{Nu} = -\int_0^1 \left[\frac{\left(\frac{\partial T}{\partial Y}\right)_{Y=0}}{T_{Y=0}}\right] dX \tag{25}$$

$$Sh_X = -X\left(\frac{\partial C}{\partial Y}\right)_{Y=0} \quad (26)$$

$$\overline{Sh} = -\int_0^1 \left(\frac{\partial C}{\partial Y}\right)_{Y=0} dX \quad (27)$$

The derivatives involved in the equations (22) to (27) are evaluated using five-point approximation formula and then the integrals are evaluated using Newton-Cotes closed integration formula.

The local skin-friction, Nusselt number and Sherwood number are plotted in figures 9, 10 and 11 respectively. Local skin-friction values for different phase angle are evaluated from equation (22) and plotted in figure 9 as a function of the axial coordinate. The local wall shear stress increases with decreasing phase angle. The trend shows that the wall shear stress is more in the case of vertical plate than horizontal plate.

The local Nusselt number for different thermal radiation parameter is presented in figure 10 as a function of the axial co-ordinate. The trend shows that the Nusselt number increases with increasing values of the thermal radiation parameter. It is clear that the rate of heat transfer is more in the presence of thermal radiation.

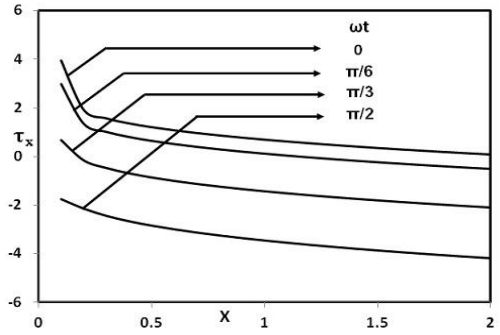

Fig. 9. Local Skin Friction.

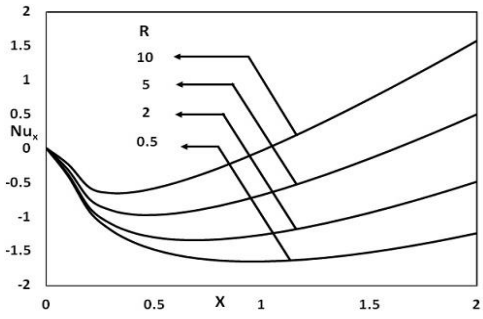

Fig. 10. Local nusselt number.

The local Sherwood number for different values of the Schmidt number are shown in figure 11.As expected, the rate of mass transfer increases with increasing values of the Schmidt number. This trend is just reversed as compared to the concentration field for different Schmidt number given in figure 8.

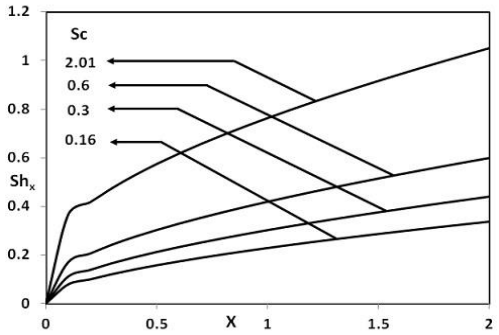

Fig. 11. Local cherwood number.

The average values of the skin-friction, Nusselt number and Sherwood number are shown in figures 12, 13 and 14 respectively. The effects of the different phase angle on the average values of the skin-friction are shown in figure 12. The average skin-friction decreases with increasing values of the phase angle.

Figure 13 illustrates the average Nusselt number increases with increasing radiation parameter. From the figure 14, it is observed that the average Sherwood number increases with increasing values of the Schmidt number.

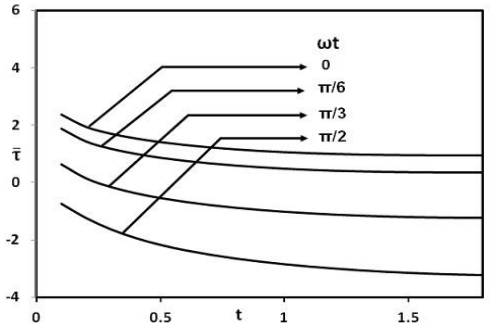

Fig. 12. Average skin friction.

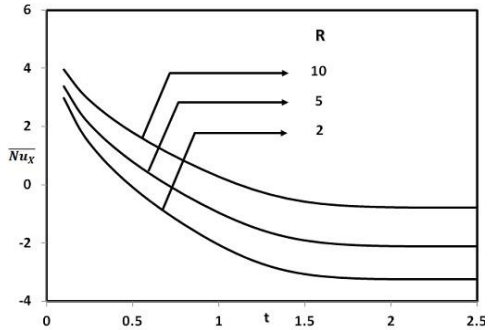

Fig. 13. Average nusselt number.

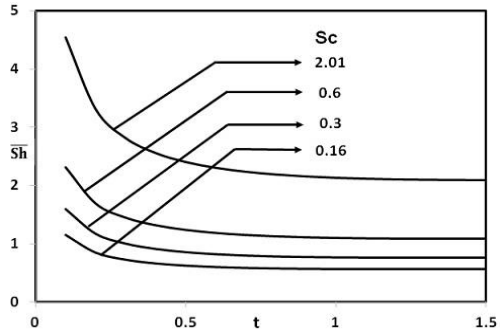

Fig. 14. Average sherwood number.

Local as well as average Nusselt number depends on temperature. It is observed that the rate of heat transfer coefficient is just opposite trend as compared with temperature profiles. The reason due to negative sign in equations (24) and (25).

Local as well as average Sherwood number depends on concentration. It is observed that the rate of mass transfer coefficient is just opposite trend as compared with concentration profiles. The reason due to negative sign in equations (26) and (27).

5. CONCLUSIONS

The numerical study has been carried out for thermal radiation effects on unsteady flow past an oscillating semi-infinite isothermal vertical plate with prescribed variable surface temperature uniform mass flux. The dimensionless governing equations are solved by an implicit scheme of Crank-Nicolson type. The effect of velocity, temperature and concentration for different parameter are studied. The local as well as average skin-friction, Nusselt number and Sherwood number are shown graphically. It is observed that the contribution of mass diffusion to the buoyancy force increases the maximum velocity significantly. It is also observed that the velocity decreases in the presence of thermal radiation. The study shows that the number of time steps to reach steady-state depends strongly on the radiation parameter and magnetic field parameter.

REFERENCES

Muthucumaraswamy R. (2009). MHD effects on flow past an infinite oscillating vertical plate in the presence of an opticallythin gray gas. *Journal of Engineering Annals of Faculty of Engineering Hunedoara* 2, 119-124.

Soundalgekar V. M., R. M. Lahurikar, S. G. Pohanerkar and N. S Birajdar (1994). Effects of Mass Transfer on the Flow Past an Oscillating Infinite Vertical Plate with Constant Heat Flux. *Thermophysic and AeroMechanics* 1, 119-124.

Soundalgekar,V. M., M. R. Patil and M. D Jahagirdar (1981). MHD Stokes problem for a vertical plate with variable temperature. *Nuclear Engg. Des.* 64, 39-42.

Soundalgekar V. M. and S. P Akolkar (1983). Effects of free convection currents and mass transfer on the flow past a vertical oscillating plate. *Astrophysics Space Science* 89, 241- 254.

Raptis, A. and C. Perdikis (1999). Radiation and free convection flow past a moving plate. *Int. J. App. Mech. and Engg.* 4, 817- 821.

W. G. England and A. F. Emery (1969). Thermal radiation effects on the laminar free convection boundary layer of an absorbing gas. *J. Heat transfer* 91, 37-44.

Soundalgekar V. M., S. K. Gupta and R. N. Aranake (1979). Free convection currents on MHD Stokes problem for a vertical plate. *Nuclear Engg. Des*. 51, 403-407.

Soundalgekar V. M., Gupta S. K. and Birajdar N. S. (1979). Effectsof Mass transfer and free convection currents on MHD Stokes problem for a vertical plate. *Nuclear Engg. Des.* 53, 339-346.

Hossian, M. A. and H. S.Takhar (1996). Radiation effect on mixed convection along a vertical plate with uniform surface temperature. *Heat and mass Transfer* 31, 243-248.

Rpatis, A. and C. Perdikis (2003). Thermal radiation of an optically thin gray gas. *Int. J.App.Mech. and Engg.* 8, 131-134.

Soundalgekar, V. M. (1979). Free convection effects on the flowpast a vertical oscillating plate. *Astrophy. and Space Sci*. 64, 165-172.

Shanker, B. and N. Kishan (1997). The effect of mass transfer onthe MHD flow past an impulsively started infinite vertical plate with variable temperature or constant heat flux. Heat and Max Transfer *Journal of Energy,* 19,.273-278.

Soundalgekar, V. M., M. R. Patil and M. D. Jahagirdar (1981). MHD Stokes problem for a vertical infinite plate with variable temperature. *Nuclear Engineering and design* 64, 39-42.

Singh, A. K. and N. C. Sacheti (1988). Finite difference analysis ofunsteady hydromagnetic free- convection flow with constant heat flux. *Astrophysics and Space Science*, 150, 303- 308.

B. Gebhart and L. Pera (1971). The nature of vertical naturalconvection flows resulting from the combined buoyancy effects of thermal and mass diffusion. *Int. J. Heat Mass Transfer* 14, 2025-2050.

Muthucumaraswamy, R. and P. Ganesan(2000). Flow past an impulsively started vertical plate with constant heat flux and mass transfer. *Computer Methods in Applied Mechanics and Engineering* 187, 79-90.

Deka, R. K. and B. C. Neog (2009). Unsteady MHD flow past a vertical oscillating plate with thermal radiation and variable mass diffusion. *Chamchuri Journal of Mathematics* 1, 79-92.

Prasad, V. R., N. BhaskarReddy, R. Muthucumaraswamy and B. Vasu (2011). Finite difference analysis of radiative free convection flow past an impulsively started vertical plate with variable heat and mass flux. Heat and Max Transfer 4 (1), 59-68.

Palani, G. and U. Srikanth (2009). MHD flow past a semi- infinite vertical plate with mass transfer. *Nonlinear Analysis Modelling and Control* 14 (3), 345456.

Prasad, V. R., N. B. Reddy and R. Muthucumaraswamy (2007). Radiation and mass transfer effects on two dimension flow past an impulsively started infinite vertical plate. *International Journal of Thermal Sciences* 46(12), 1251-1258.

Chandrakala, P. and P. N. Bhaskar (2009). Thermal radiation effects on MHD flow past a vertical oscillating plate. *International Journal of Applied Mechanics Engineering* 14(2), 349-358

Rajput, U. S. and S.Kumar (2011). MHD flow past an impulsively started vertical plate with variable temperature and mass diffusion. *Applied Mathematical Sciences* 5(1-4), 149-157.

Chaudhary, R. C. and A. Jain (2007). Unsteady free convection flow past an oscillating plate with constant mass flux in the presence of radiation. *Acta Technica CSAV* 52(1), 93-108

Muthucumaraswamy, R. and A. Vijayalakshmi (2008). Effects of heat and mass transfer on flow past an oscillating vertical plate with variable temperature. *Internatioinal Journal of Applied Mathematics and Mechanics* 4, 59-65

B. C. Neog and K. R. Das Rudra (2012). Unsteady Free Convection MHD flow past a vertical plate with variable temperature and chemical reaction. *International Journal of Engineering Research and Technology* 1, 1-5.

Rajput, U. S. and S. Kumar (2012). Radiation effects on MHD flow past an impulsively started vertical plate with variable heat and mass transfer. *International Journal of Applied Mathematics and Mechanics* 8, 66-85

Carnahan, B., H. A. Luther and J. O. Wilkes (1969). *Applied Numerical Methods*. John Wiley and sons, New York.